Nuclear Engineering and Technology 55 (2023) 1671–1676

Contents lists available at ScienceDirect

Nuclear Engineering and Technology

journal homepage: www.elsevier.com/locate/net

Original Article

Simulating the impact of iodine as a contrast substance to enhance radiation to the tumor in a brain x-rayphototherapy

M. Orabi

Physics Department, Faculty of Science, Cairo University, Giza, 12613, Egypt

ARTICLE INFO

Article history:
Received 7 March 2022
Received in revised form
5 October 2022
Accepted 2 January 2023
Available online 2 January 2023

Keywords:
Ionizing radiation
X-rays
Phototherapy
Monte-carlo
Contrast substance
Brain cancer
Iodine

ABSTRACT

The influence of adding iodine as a contrast substance to elevate radiation in a tumor is studied using simulation techniques of Monte-Carlo. The study is carried on a brain cancer by adopting an unsophisticated head phantom. The ionizing radiation source is an external beam of x-rays with energy range of a few tens of keV. The expected radiation dose increment due to adding the iodine is investigated by comparing the radiation in the tumor after and before adding the iodine and calculating the ratio between the two doses. Several concentrations of the contrast substance are used to quantify its impact. The change of the dose increment with the source energy is also examined. It is found that the radiation elevation in the tumor tends to saturate with increasing the iodine concentration, and for the studied domain of energies (30 keV–100 keV), the radiation dose enhancement factors (RDEF) for the different iodine concentrations (1%–9%) show peaked curves, with the peak occurring between 60 keV and 70 keV. For the highest concentration studied, 9%, the peak value is almost 7.

1. Introduction

Radiation is used as much in therapy as in imaging. Several cancer cases can be cured by radiation treatments, in particular those localized ones that are discovered early before the cancer spreads [1–3]. In addition, radiation treatments can be applied as subsidiary operations to help stop the cancer from coming back after it is cured by surgical or chemical treatments. The physical idea behind applying radiation in cancer therapy is that it can be used to wipe off the unwell tissues by depositing enough energy into them. This of course indicates the criticality in conveying the radiation to the cancer area, and what that entails in selecting the type of radiation, its energy, intensity, and rate to impinge. In addition to all of that, it is very vital that the other well areas around the cancer to be kept protected as much as possible from receiving radiation. In this research article we concern about this point when conveying radiation for treating cancer. It simulates and discusses a technique for condensing the radiation on the cancer area, to sharpen the treatment, while at the same time keeps the other well areas as protected as possible.

Based on the place of the source, radiation treatments can be categorized into two types; internal and external radiotherapies [4]. In the first category, the radiation source is placed inside the human body. This category itself is branched into two sets; a) a systematic set with unsealed radiation sources in the form of components called radiopharmaceuticals, and b) the brachytherapy set with sealed radiation sources manufactured as seeds covered by titanium. An example of set (a) is the use of rhenium-188 labeled radiopharmaceuticals for medullary cancer [5]. The other set (b) is usually applied for localized cancer like in head, neck, breast, eye and prostate [6–8]. The number and type of seeds used depend on dose rate intended, the position of the cancer and its condition. For LDR prostate cancer brachytherapy, for example, an average number of 100 iodine-125 seeds is used [9]. For the second category, the external radiotherapy, the radiation source is outside the body. A radiation beam from an external tool is aimed at the body in a way that tries to focus the radiation on the cancer region. Usually, a multiple number of beams are incident from different angles to lower the radiation dose gotten by the well areas around the cancer region. One important class of the second category is to use an external x-ray beam [10]. Other types of beams can also be used like for example electron and proton beams as demonstrated in references [11,12]. Both these articles are Monte-Carlo studies; in the first one they study the use of focused very-high-energy electron beams to treat deep-seated tumors, while in the second paper they

E-mail addresses: momen_ahmad_orabi@cu.edu.eg, momenorabi11@gmail.com.

https://doi.org/10.1016/j.net.2023.01.003

investigate the possible damage that could happen by secondary radiation to the surrounding organs when using a proton beam for breast cancer therapy. Here in this article, we are interested in studying external beam radiotherapy with kilo voltage x-rays, in which the directed beam of photons has energies in the range of few tens of keV. This would be guessed to be less effective than using mega voltage photons, especially with deeply located cancer regions that cause a high weakening of the photons before reaching the target and accordingly causes a high reduction to the dose. Although this image might be correct, it could however be altered by doping the cancer region with a high-atomic-number substance, which is named a contrast substance. This mechanism is known as x-ray phototherapy. With the photon energies in the range of keV, the contrast substance is expected to promote the photoelectric effect interactions within the cancer region, leading to higher radiation doses there [13,14]. This would have a one promising advantage over using mega voltage photons, which is that the well areas around the cancer region will be spared from having excessive radiation doses.

Implementing an x-ray phototherapy will entail many points to be considered. For example, the radiotherapist will have to select the proper x-ray spectrum to be used. In other words, selecting the energy spans and their strengths. In a related matter, the rate of conveying the radiation dose has to be decided, which is also controlled by the type of the contrast substance to be used and its concentration. All these factors are in fact controlled by the determined total amount of radiation dose that needs to be conveyed to the cancer area. Inspecting each of the involved points requires a great deal of experimental tests, which practically is very tedious. Something to comfort these studies is to rely on simulation work. It is a very powerful tool that can efficiently ease the experimental studies and extremely save time, effort and costs. Of course the experimental work has to be done eventually, but with the guidance of the simulation results, a big difference is made. This is one of the essential points of this kind of studies as presented in this paper. Here we offer an important part of simulation results that could show the potential that may be found in the x-ray phototherapy as applied in the case of brain cancer, as an example. This work, among other simulation works, is to enrich the medical physics and radiotherapy theoretical studies.

The Monte Carlo software MCNP5 [15] will be used to construct the required codes to carry out the simulation work. It has powerful abilities in performing simulations of different varieties to calculate the radiation doses and perform several analyses [16,17].

2. Materials and method

2.1. Human head representation

The description of the head has to account for both its dimensions and structure. The exact shape of the head may be very crucial in some studies, but in ours here it is not thought to be so. Therefore, an unsophisticated model is taken for the human head to depict its basic dimensions and structure in adults [18,19]. The head is taken as a sphere of 18 cm diameter. To border the different parts in the head, a series of central spheres are used. After the outside sphere there is one with diameter 17.5 cm. This determines the skin region with thickness 0.25 cm. After that comes a sphere with diameter 16 cm to determine the skull region as having a thickness 0.75 cm. The remaining space inside the 16 cm diameter sphere is taken as the brain with the cancer region assumed to be located in the central core as a sphere with diameter 4 cm. A schematic graph of the head phantom is shown in figure (1). The numbers between the parentheses in the figure are the thicknesses. The chemical structures of the different parts in the head are taken from Ref. [19]. That of the brain, for example, is provided in table (1). The ZAID number for each of the elements in the tumor composition, and their weight percentages, are given in the table. The ZAID number (Z A IDentification) is composed of six digits; the first three are the atomic number and the second three are the mass number [20,21]. For oxygen, for example, it is 008016, or simply 8016. The negative numbers in the table indicate that weight fractions are used and not atomic abundances. The sum of the weight fractions is not 1, as supposed to be, because not all the elements are shown in the table, but just the main ones. When a contrast substance is included, these numbers are renormalized to accommodate the percentage contribution from the contrast substance and still get the final sum equals to 1.

2.2. Radiation source and geometry description

The source of radiation used in this study is a tube of x rays that has a tungsten target and works at a potential difference 100 kV. This external source provides a continuous spectrum of photon energies that span values from just few eV up to 100 keV. This is displayed in figure (2). This spectrum is just the output of a device and only used in the simulation codes. Moreover, only the major areas in the spectrum are presented on the figure. In addition to the continuous spectrum, there are line parts in the spectrum that are characteristic of the target, the tungsten, caused by de-excitation between its energy levels. With this x-ray tube, the line parts are mainly two lines, the K_α and K_β, which are shown in figure (2) as two crests at energies around 60 keV and 70 keV, respectively. The x-ray beam in the simulation programs has a radius of 4 cm and its opening is at a distance 3 cm above the head [22], and there is air between the x-ray tube and the head phantom. The density of the air is taken as 0.0013 g/cm^3, while those for skin, skull and brain are 1.09 g/cm^3, 1.61 g/cm^3 and 1.04 g/cm^3, respectively.

2.3. Physics interpretation and tally choice

Having the above-described source of radiation with its extent of photon energies, the cross-section of the photoelectric effect will be the highest among other interactions cross-sections like Compton scattering for example. The photoelectric cross-section rises more in the cancer region by doping it with a contrast substance. This is the basic objective behind applying an iodine-based substance; to distinguish the cancer region by marking it with a high-Z substance. This multiplies the interaction probability of the photoelectric effect inside the cancer region, which leads to extra radiation there caused by secondary interactions involving photoelectrons, auger electrons and characteristic x-rays. Consequently, the absorbed radiation dose to the cancer region is leveled up.

It is clear from the physical explanation of how the contrast substance helps in elevating the radiation dose to the cancer region

Table (1)
ZAID numbers of the elements in the tumor composition together with their weight fractions. The negative numbers indicate that weight fractions are used and not atomic abundances. The sum of the weight fractions is not 1, as supposed to be, because not all the elements are shown in the table, but just the main ones. When a contrast substance is included, the fractions are renormalized to accommodate the percentage contribution from the contrast substance and still get the final sum equals to 1. This chemical composition of the brain as given here is in accordance with the ICRU report no. 46 [19].

Element	ZAID number	Weight percentage
Hydrogen	1001	−0.107
Carbon	6012	−0.145
Nitrogen	7014	−0.022
Oxygen	8016	−0.712

Table (2)
RDEF in the cancer region of the brain calculated at several sets of the source energy and iodine concentration. The energies are in keV.

Iodine concentration	E = 30	E = 40	E = 50	E = 60	E = 70	E = 80	E = 90	E = 100
1%	1.28	1.92	2.26	2.33	2.24	2.09	1.94	1.78
3%	1.67	2.78	3.74	4.14	4.04	3.80	3.46	3.11
5%	1.90	3.14	4.52	5.26	5.34	5.08	4.67	4.18
7%	2.05	3.31	4.95	6.01	6.26	6.07	5.64	5.09
9%	2.16	3.41	5.22	6.50	6.94	6.86	6.44	5.85

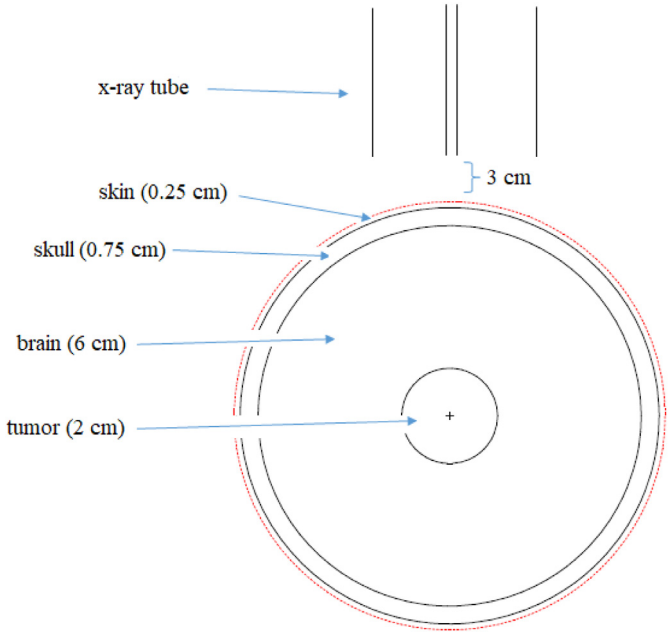

Figure (1). The simulation geometry as described in the MCNP5 codes. The plus sign in the middle of the figure is the origin of the coordinates. The head phantom picture is taken from the MCNP5 graphics of the input file. The numbers between the parentheses are the thicknesses.

that it is very vital that we involve both the photons and electrons interactions when tallying the radiation inside the cancer region. This hints that the right tally for this job is the f8 one because of its available option of calculating the radiation height by including the photons and electrons, and not just one of them as in the case of the tally f4. The tally f8 calculates the radiation spectrum inside some volume. Here in this research, we shall utilize it to analyze the radiation spectrum, caused by photons and electrons, as being pushed up inside the cancer region. For the sake of fine resolution, the particle's energy in the spectrum is going by a pace of 1 keV. Additionally, a big enough history number, 10^8, is taken in the codes to guarantee a sufficient accuracy. The contrast substance is assumed to be spread uniformly throughout the tumor, and it is concentration is represented as a percentage of the mass composition of the tumor.

3. Results & discussion

To play its role of making the cancer region in the brain of higher dose rate than the remaining brain regions, it is very essential that the contrast substance to be put in the cancer region only and nowhere outside of it. In doing the simulation work here, this is taken to be the case. The contrast substance considered in this study is an iodine-based one. In practice, the contrast substance is a mixture of a number of elements to make it safe to be taken in by the human body. However, only one element in that mixture is important for doing the job of the contrast substance, and that element is the one having high-Z. To account for the contrast substance in the cancer region, it is not necessary to include all the elements of its structure; the important thing is to include the high-Z element. This is an approximation, which is quite acceptable, and it simplifies very much the way of representing the cancer region as doped with the contrast substance. More specifically this is taken by using the weight-fraction of the iodine as a representative for the contrast substance concentration inside the cancer region.

Having the above described simulation setup, we get figure (3), which demonstrates the rise of radiation in the cancer region caused by the existence of iodine (Z = 53). The spectrum is presented for just its most prominent portions where the energy varies roughly between 30 keV and 70 keV. If the energy is smaller or bigger, the spectrum exhibits some sort of oscillations that are caused by the lowered fluence of particles. The spectra in figure (3) are calculated by supposing that the contrast substance is spread evenly throughout the cancer region. Concentrations of iodine in the graph are 0%, 1%, 3%, 5%, 7% and 9%, from the lowest curve to the highest one, respectively.

Although, as one can observe from figure (3), that the radiation in the cancer region keeps rising as the concentration of the iodine keeps getting higher, this trend is restricted. If we look carefully

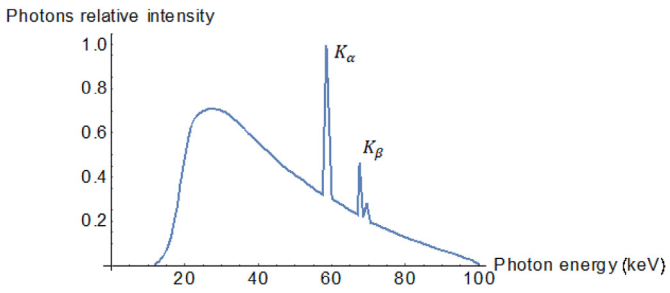

Figure (2). Energy spectrum of the x-rays. The tube has a tungsten target and voltage 100 kV. Only the major regions in the spectrum are presented. The K_α and K_β crests (left and right, respectively) are the tungsten characteristic x-rays.

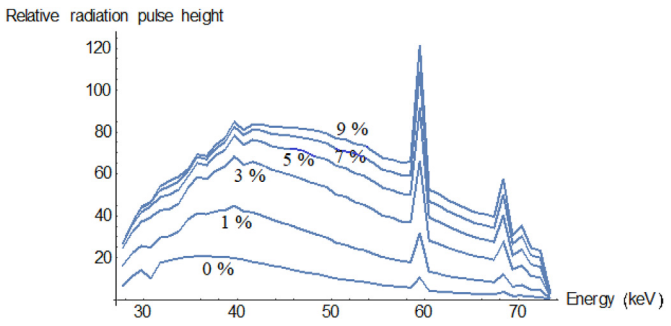

Figure (3). Radiation rise in the cancer region of the brain by adding iodine-based contrast substance. Iodine concentrations are 0%, 1%, 3%, 5%, 7% and 9% from the lowest curve to the highest. The source photons energy spectrum is that of figure (2).

into the curves in figure (3), we can notice that the distances among them are getting smaller and smaller as the curves go higher and higher. This takes place while the concentration of iodine is changing by a constant pace, as shown in the figure. What happens is that, at first, the radiation level in the cancer region rises quickly by adding iodine, but after a while that rise slows down, and if this goes on there will be no rise in the radiation anymore, and in fact it might tend to decrease. All this occurs due to the self absorption process that is caused by adding a big enough amount of the contrast substance to the extent that it may start to act as an absorber and take in some of the developed radiation.

Before we discuss the radiation increment further, we first put a definition for the RDEF. This is the radiation dose to a certain volume in the body after using a contrast substance divided by the radiation dose to the same volume and under the same conditions but without using the contrast substance. Considering the RDEF for the cancer region, it can be speculated from figure (3) to be controlled not just by the contrast substance concentration but by the particles energies as well. To show this in a clearer form, we replace the x-ray source with a hypothetical source of photons having a single energy and see how the radiation elevation will behave at the different iodine concentrations. Figure (4) illustrates such behavior for photons of energy 50 keV. As with the continuous-spectrum source, the radiation keeps elevating, as the iodine concentration keeps getting higher. Moreover, the process of self absorption also occurs. The same behaviors are also witnessed in figure (5) where an energy of 60 keV is considered. The two energies 50 keV and 60 keV are compared to each other in figure (6) at a given value of the iodine concentration, which is 3%.

Graphs (3), (4) and (5) demonstrate how the radiation elevation is highly controlled by the contrast substance concentration and by the source energy. To demonstrate this further, the RDEF for the cancer region is calculated for a number of iodine concentrations and photon energies. The results are shown in table (2). The concentrations in the table vary from 1% to 9% in step of 2%, while the energies vary from 30 keV to 100 keV in step of 10 keV. From this table it can be seen that the RDEF for the cancer region increases to reach a maximum value, after which it starts to decline. To see this in a better way, we provide a graphical form for table (2) in figure (7). This behavior happens because with increasing the energy beyond some limit, the photoelectric effect becomes less dominant, and accordingly the absorption difference between iodine and the soft tissues becomes less optimum.

The graphs in figure (6) may look in contradiction with the results in table (2), because the graph corresponding to 50 keV is higher than that of 60 keV. However, this does not mean that the energy 50 keV has a higher RDEF than the energy 60 keV, because if one looks carefully into figure (6), it can be realized that the energy

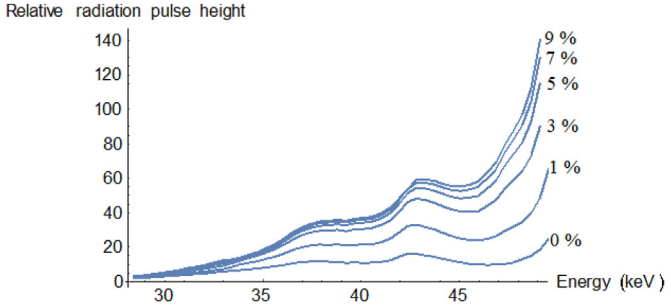

Figure (4). Radiation rise in the cancer region of the brain by adding iodine-based contrast substance. Iodine concentrations are 0%, 1%, 3%, 5%, 7% and 9% from the lowest curve to the highest. The source photons energy is 50 keV.

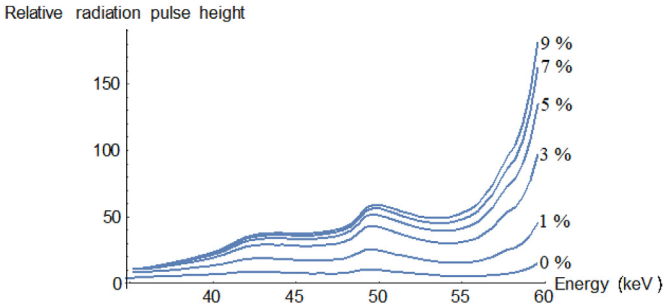

Figure (5). Radiation rise in the cancer region of the brain by adding iodine-based contrast substance. Iodine concentrations are 0%, 1%, 3%, 5%, 7% and 9% from the lowest curve to the highest. The source photons energy is 60 keV.

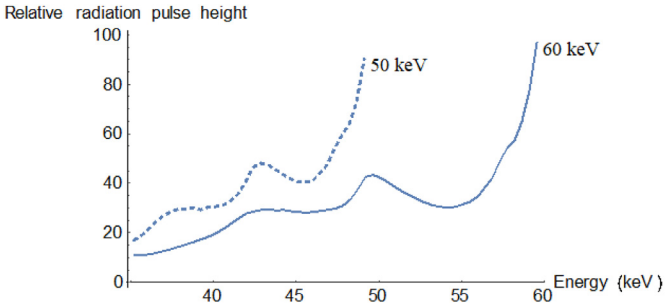

Figure (6). Radiation rise in the cancer region of the brain by adding iodine-based contrast substance. The dashed curve which corresponds to the source energy 50 keV is compared to the solid curve corresponding to the source energy 60 keV. Iodine concentration is 3 %.

60 keV has a wider spectrum than that of 50 keV, and therefore if we perform an integration over the whole spectrum, it is obvious that 60 keV will have a higher RDEF than that of 50 keV. The spectrum is higher for 50 keV because for this energy the cross-section of the photoelectric effect is higher than that for the energy 60 keV.

The results in table (2) also indicate an interesting remark about the increase of the radiation intake by the cancer region; the initial dose before adding the contrast substance may get multiplied by a factor up to almost seven. This of course depends on the energy spectrum of the source and the concentration of the contrast substance, but it clearly shows how much the inclusion of the contrast substance can make a difference.

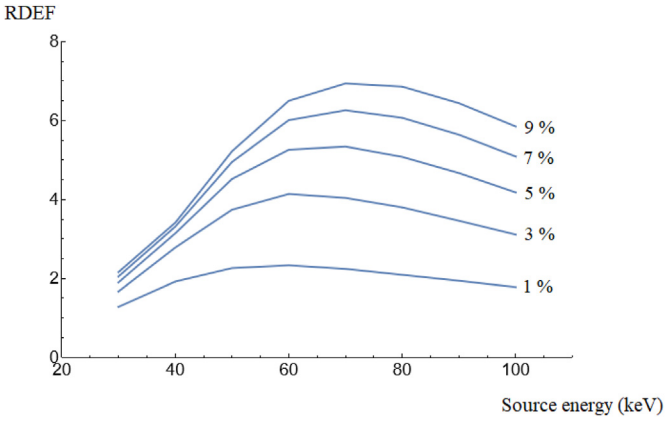

Figure (7). RDEF as a function of the source energy for different iodine concentrations.

As a validation for our simulation model, we compare its results with other studies. First, we consider the experimental results of ref [23] where they use iodine nanoparticles as a dose-enhancing agent for radiotherapy of mice brains having cancer that is taken from human breast. In that study, they use an x-ray spectrum of a 100 kV source and iodine nanoparticles concentration of 7 g iodine/kg body weight to get an approximate 5.5 dose enhancement. To compare with their result, we first have to find the corresponding concentration in our model. A concentration of 7 g iodine/kg body weight means that for a typical mouse body weight of 20 g, it will take 0.14 g of iodine. Knowing that for rodents the brain-to-body mass ratio is about 1–40 (~2.5%), which would mean that the 20 g mouse will have about 0.5 g brain. Dividing 0.14 g iodine by 0.5 g brain gives 0.28 or 28%, which is the concentration of iodine in our model. Using this concentration with our 100 kV x-ray source, we get a dose enhancement of 6.32, which is in a good agreement with that of ref [23], namely 5.5. In fact, experimentally not all the injected iodine is really taken in by the target, because not all the injected iodine stays confined within the tumor. This means that the theoretical representation of the concentration should actually be less than 28%. Assuming, for example, that out of the 0.14 g of iodine only 0.1 g stays inside the tumor, this will give a concentration 20%, which results in a dose enhancement of 6.10; a closer number to Ref. [23] with only difference 10%. It is important to note that the results obtained are not dependent on the body mass of the mouse.

Second, we consider ref [24] which uses the MCNP4A code to calculate the dose distribution in a cancer treatment by kilovoltage x-rays delivered from a computed tomography scanner with the application of multiple arcs. In their results they show a relation between the dose enhancement and the source energy for different iodine concentrations. For convenience of the reader, we show their graph in figure (8). This could be compared to figure (7). As can be seen, the two figures (7) and (8) show similar behaviors. In both figures the curves are higher by increasing the iodine concentration, and they are denser at lower energies than at higher ones. In figure (7), because we have a fixed step of increasing the concentration, we can say that the gaps between the curves are getting less by increasing the concentration, but in figure (8) we cannot comment about that because the step 15 mg I/ml is missing. It should be emphasized that, in our calculations, the concentration 5%, for example, does not correspond to the concentration 5 mg I/ml in Ref. [24]. Unfortunately, with the way they consider iodine concentration, a connection between their numbers and ours is not clear. Despite the similarity between the two figures (7) and (8), still there are some differences. For example, in figure (8), independent of the concentration, all the curves are peaked around the energy 50 keV (or at least for their studied concentrations). In figure (7) however, the energy at which the peak occurs shifts from lower energies at lower concentrations to higher energies at higher concentrations. Moreover, the curvature shape of the curves is slightly different in the two figures. In addition to the different geometries and model structures between this study and ref [24], the variations in the results are expected to be mostly due to the different cross-section libraries used by the different Monte-Carlo codes.

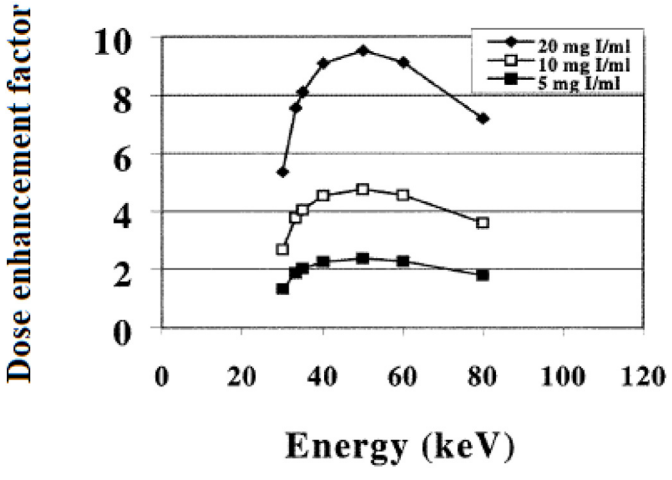

Figure (8). Dose enhancement factor as a function of the energy for different iodine concentrations as taken from Ref. [24].

4. Conclusion

The x-ray phototherapy has been studied using the MCNP5 program with a plain description for the human head with a brain cancer. Iodine-based contrast substance is applied by taking the iodine as a representative for the substance. The existence of iodine in the tumor causes a rise in the radiation there by fluxes of secondary particles. Sources of photons with continuous- and line-energy spectra have been used and analyzed. For the studied range of energies, tens of kilo-electron-volt, the RDEF was found to have a peaked value spanned over 60–70 keV. The peak for the lowest concentration (1%) is about 2.33, occurring around 60 keV, while for the highest concentration (9%) it is about 6.94, occurring around 70 keV. For changing the concentration, it was found that the radiation elevation in the tumor keeps going up with increasing the iodine concentration until saturation happens due to self absorption.

The presented results illustrate the potential of using the x-ray phototherapy as one of the methods of radiation therapy for curing different cancer types. One of the important goals when performing a radiotherapy process is to decrease the treatment period. While this could sometimes be accomplished by using higher photon energies (mega-voltage range), it would be at the cost of increasing the chance of harming the healthy tissues around the tumor. The technique simulated in this article is expected to be a relief for that issue as it uses x-rays in the kilo-voltage range with enhancing the radiation only in the marked area, namely the cancer region. However, it should be emphasized that the results here are demonstrating the case from a theoretical point of view, assuming the contrast substance be administered only to the tumor, and it is spread uniformly there. Practically, however, this might not be the case.

The work performed in this study is considered a basis for more sophisticated works that can be carried out by developing some parts in the codes and by including x-ray phototherapy as part of a whole therapy process that involves more than one kind of treatment like surgery and chemotherapy. This can also be upgraded by including calculations of the build-up factors, such as the exposure build-up factor and the energy absorption build-up factor, which have a significant role in photons dispersion and dose calculations [25]. Moreover, it will be interesting to perform a study that deliberately compares between the current results and when using iodine as nanoparticles in different sizes under the same simulation setup and conditions [26,27]. Some of these ideas are in progress.

Declaration of competing interest

The authors declare that they have no known competing financial interests or personal relationships that could have appeared to influence the work reported in this paper.

References

[1] C.K. Bomford, I.H. Kunkler, Walter and Miller's Textbook of Radiation Therapy, sixth ed., 2003, p. p311.
[2] M.M. Khalil, Basic Sciences of Nuclear Medicine, Springer international publishing, 2021, pp. 3–27, https://doi.org/10.1007/978-3-030-65245-6.
[3] https://en.wikipedia.org/wiki/Radiation_therapy. Last visited in October 2022.
[4] C.M. Washington, D. Leaver, Principles and Practice of Radiation Therapy, fourth ed., Elsevier, 2016.
[5] N. Lepareur, et al., Rhenium-188 labeled radiopharmaceuticals: current clinical applications in oncology and promising perspectives, Front. Med. 14 (6) (2019) 132.
[6] R. Bhalavat, et al., Brachytherapy in head and neck malignancies: Indian Brachytherapy Society (IBS) recommendations and guidelines, J. Contemp. Brachytherapy 12 (5) (2020) 501–511.
[7] V. Khetan, et al., Brachytherapy of intra ocular tumors using 'BARC I-125 OcuProsta seeds': an Indian experience, Indian J. Ophthalmol. 62 (2) (2014) 158–162.
[8] J. Skowronek, A. Chichel, Brachytherapy in breast cancer: an effective alternative, Prz Menopauzalny 13 (1) (2014) 48–55.
[9] E.T.T. Leite, et al., Prostate brachytherapy with iodine-125 seeds: analysis of a single institutional cohort, Int. Braz J. Urol. 45 (2) (2019) 288–298.
[10] D.Y. Breitkreutz, et al., External beam radiation therapy with kilovoltage x-rays, Phys. Med. 79 (2020) 103–112.
[11] K. Kokurewicz, et al., Focused very high-energy electron beams as a novel radiotherapy modality for producing high-dose volumetric elements, Sci. Rep. 9 (2019), 10837.
[12] N. Azadegan, et al., Calculation of secondary radiation absorbed doses due to the proton therapy on breast cancer using MCNPX code, Radiat. Phys. Chem. 183 (2021), 109427.
[13] J.P. Gibbons, et al., Khan's the physics of radiation therapy, J. Med. Phys. 45 (2) (2020) 134–135.
[14] W.R. Leo, Techniques for Nuclear and Particle Physics Experiments, second ed., Springer-Verlag, 1994, pp. 53–62.
[15] MCNP5 - a General Monte Carlo N-Particle Transport Code, Los Alamos National Laboratory, 2005. Version 5.
[16] M. Orabi, O. Abdurahem, M. Sherif, Utilizing Monte Carlo computations to estimate radiation doses from some cosmetics, Health Phys. 115 (3) (2018) 382–386.
[17] M. Orabi, Studying factors affecting the indoor gamma radiation dose using the MCNP5 simulation software, J. Environ. Radioact. 165 (2016) 54–59.
[18] https://en.wikipedia.org/wiki/Human_head. Last visited in September 2022.
[19] ICRU (International, Commission on Radiation Units and measurements). Photon, electron, proton and neutron interaction data for body tissues, Report no 46 (1992).
[20] M. Hassanpour, et al., Studies of the mechanical and neutron shielding features of concrete by incorporation of green additive materials: experimental and numerical study, Radiat. Phys. Chem. 191 (2022), 109846.
[21] Manual of the MCNP5 - a General Monte Carlo N-Particle Transport Code, Los Alamos National Laboratory, 2005. Version 5.
[22] D.Y. Breitkreutz, M.D. Weil, M. Bazalova-Carter, External beam radiation therapy with kilovoltage x-rays, Phys. Med. 79 (2) (2020) 103–112.
[23] J.F. Hainfeld, et al., Iodine nanoparticle radiotherapy of human breast cancer growing in the brains of athymic mice, Sci. Rep. 10 (2020), 15627.
[24] A.V. Mesa, et al., Dose distributions using kilovoltage x-rays and dose enhancement from iodine contrast agents, Phys. Med. Biol. 44 (1999) 1955–1968.
[25] Ö. Eyecioğlu, et al., BXCOM: a software for computation of radiation sensing, Radiat. Eff. Defect Solid 174 (5–6) (2019) 506–518.
[26] R. Delorme, et al., Comparison of gadolinium nanoparticles and molecular contrast agents for radiation therapy-enhancement, Med. Phys. 44 (11) (2017).
[27] B. Bilmez, et al., Monte Carlo study on size-dependent radiation enhancement effects of spinel ferrite nanoparticles, Radiat. Phys. Chem. 199 (2022), 110364.